

Vibronic coupling and the near-infrared spectrum of Fe^{2+} in CdTe and ZnS

Juan Rivera-Iratchet and Manuel A. de Orúe

Departamento de Física, Facultad de Ciencias, Universidad de Concepción, Concepción, Chile

Eugenio E. Vogel

Departamento de Ciencias Físicas, Facultad de Ingeniería, Universidad de la Frontera, Temuco, Chile

(Received 28 January 1986)

The main characteristics of the near-infrared spectrum of Fe^{2+} in both CdTe and ZnS are attributed to vibronic coupling between the $3d^6$ configuration of Fe^{2+} and the local vibrations induced by the lattice dynamics. A strategy is devised to obtain the quantitative aspects of the coupling (coupling energy and energy of the coupling mode) from the low-energy zero-phonon absorption lines. The calculation includes the diagonalization of a Jahn-Teller Hamiltonian with respect to a number of wave functions that depends on the number N of vibrational quanta. Numerical results are obtained for the intensities of the absorbed lines and energies of the absorbed photons that are in good agreement with experiments. The values of the two free parameters also are in good agreement: the energy of the coupling phonon is the expected one in accordance with the lattice dynamics of both CdTe and ZnS; the value of the Jahn-Teller energy is in correspondence with previous estimates. The method is simple and easy to use for other similar systems. The convergence with respect to N is also studied and found to give reproducible results for $N=10$ in the case of CdTe; the convergence for ZnS is actually faster than that for CdTe.

I. INTRODUCTION

The infrared-absorption spectra of Fe^{2+} ion in cubic II-VI compounds have been known for about two decades. In particular the cases of CdTe: Fe^{2+} and ZnS: Fe^{2+} received considerable attention both experimentally and theoretically.¹⁻⁶ Crystal-field theory is not sufficient to explain the experimental results. The Jahn-Teller (JT) effect has been found important in the far-infrared spectrum of Fe^{2+} in CdTe and negligible for Fe^{2+} in ZnS.^{7,8} However, no quantitative approach has accounted for the near-infrared spectra of Fe^{2+} in ZnS, CdTe, and other zinc-blende structure compounds. We attempt here to explain part of the spectrum, namely, the first few zero-phonon absorption lines, as a way to gain quantitative information about the vibronic coupling in these systems.

The method is based on the diagonalization of a Hamiltonian which includes a linear JT coupling. In doing so we continue along the line which has been already used for other similar systems.⁹⁻¹¹ The existence nowadays of large and powerful computers makes this method extensible to include vibronic states with a large number of vibrational quanta which was impossible at the time the first explanations of the spectra were attempted.

The lattice dynamics of zinc-blende compounds was studied in the comprehensive work of Kunc.¹² The compounds of our particular interest were thereafter studied both experimentally and theoretically.¹³⁻¹⁵ Quite recently different techniques have made possible extensive calculations that allow reliable interpretations of the experimental data.¹⁶⁻¹⁹ This is encouraging in the sense that once the vibronic mechanism is well established, the whole near-infrared spectrum could be drawn according to *ab initio* calculations.

The aim of the present article is to find a way to use the simplest part of the near-infrared absorption spectrum in order to describe the vibronic coupling in a quantitative manner. If we compare the spectra of Fe^{2+} in different zinc-blende compounds we realize that there is one striking difference that cannot be attributed to crystal-field symmetry or spin-orbit coupling, which is basically the same for all of them: the first few zero-phonon lines show a quite distinct distribution of the intensities within the first 50 cm^{-1} (or less) as measured from the lowest-energy absorption line. We think this is the fingerprint of the unique physical aspect of Fe^{2+} in all these compounds, namely the vibronic coupling. In the rest of the article we develop a strategy to bring out the maximum amount of information about the coupling mechanism from the low-energy part of the near-infrared spectrum.

In Sec. II we make a review of the most important aspects of the experimental information for both CdTe: Fe^{2+} and ZnS: Fe^{2+} . In Sec. III we give a brief account of the general theory and some particular considerations for our problem. In Sec. IV we discuss the strategy to perform the calculations analyzing the different implications for both CdTe and ZnS. In Sec. V we give the main results of the calculations in the form of graphs; we also discuss the results and compare with experiments and previous theoretical calculations. In Sec. VI we conclude that the method gives good and consistent results; we also discuss the possible extensions of this work.

II. REVIEW OF EXPERIMENTAL RESULTS

We shall concern ourselves here with the low-temperature near-infrared spectra of Fe^{2+} in both CdTe and ZnS. Generally speaking the absorption spectra of

TABLE I. Summary of some experimental results for Fe^{2+} in CdTe and ZnS. In the upper part we present the energies $h\nu$ and approximate relative intensities f_i/f_0 of the absorbed lines. (One line is assigned an intensity f_0 so the ratios can be immediately established.) In the lower part we present the most important values for the phonon energies of the acoustic branches. (Parentheses around the relative intensities indicated possible phonon-assisted lines according to previous interpretations.)

CdTe		ZnS	
$h\nu$ (cm^{-1}) ^a	Absorption lines		f/f_0 ^b
	f/f_0 ^b	$h\nu$ (cm^{-1}) ^c	
2282	1	2945	8
2294	1	2964	1/3
2309	1	2984	1/5
2318	($\frac{1}{4}$)	3051	(1)
2334	($\frac{1}{4}$)	3129	(2)
2346	($\frac{1}{4}$)		
Phonon energies			
	$\hbar\omega$ (cm^{-1}) ^d		$\hbar\omega$ (cm^{-1}) ^e
TA(X)	35	90	
TA(L)	29	70	
TA ₁ (K)	37	120	
TA ₂ (K)	53	87	
LA(X)	120	211	
LA(L)	108	195	

^aReference 5.

^bReference 1.

^cReference 6.

^dReference 13.

^eReference 14.

Fe^{2+} in several II-VI compounds⁴ show a sharp rise to one, two, or three narrow lines in the region around 2000–3000 cm^{-1} . Beyond these zero-phonon lines a complicated structure is observed in the form of broad lines probably due to phonon-assisted transitions.

In the case of Fe^{2+} in CdTe^{1,5} three narrow lines are observed at 2282, 2294, and 2301 cm^{-1} . The sharpness of these lines is an indication of zero-phonon transitions. One interesting feature is that the oscillator strength is roughly the same for these three lines; this fact will be fundamental in the model calculation to be performed later. A few other possible zero-phonon lines are also seen although the oscillator strength is significantly smaller than the one corresponding to the first three lines; it is not clear whether some of these lines are phonon-assisted transitions. On the other hand, the phonon-dispersion curves for CdTe are known and theoretical calculations show good understanding of the corresponding lattice dynamics.^{13,17,19}

A different picture is shown by Fe^{2+} in ZnS.^{1,3,6} Just one narrow line is observed at 2945 cm^{-1} with an intensity much larger than any other zero-phonon line of the spectrum. However, weaker lines are seen at 2964, 2984, 3051, and 3129 cm^{-1} . Qualitative arguments have been given in order to interpret these lines. The phonon dispersion curves of ZnS are experimentally known¹⁴ and

theoretical models^{16,18,19} are in good agreement with them, thus giving reliable values for the energies of the phonons capable of producing vibronic coupling.

In Table I we present a summary of the most relevant experimental features of CdTe, ZnS, and the role of Fe^{2+} in these two crystals from the point of view of the aim of the present paper.

III. THEORY

The localized 3d electrons of Fe^{2+} are sensitive to vibrations of the surrounding atoms; this is so even at very low temperatures due to the zero-point energy of the phonons. From the start we ignore long-wavelength phonons as they do not lead to significant relative displacements among nearest neighbors.

As a short-wavelength phonon passes by the site of an iron impurity the four nearest-neighbor anions (S, Te, . . .) vibrate in a way that can be understood as a superposition of the nine independent vibrational modes of a tetrahedron.²⁰ (This is sometimes called the cluster model.) In terms of the irreducible representations corresponding to the point group T_d they can be written as $A_1 + E + T_2^a + T_2^b$. The “breathing” mode A_1 does not lead to admixture of electronic wave functions, and hence cannot be responsible for extra lines in the optical spectra. It has been found that in similar systems^{6,10} the coupling to E modes alone explains qualitatively at least most of the characteristics of the first few infrared lines. We will adopt this model for simplicity. We must point out, however, that at least one of the two T_2 modes could couple to the iron electrons with phonons of about the same energy as those that lead to the coupling to E modes (the coupling energy could be quite different). The approximation just described relays two facts: (a) If E modes are not enough to explain the experimental data we can recover T_2 modes and expand the basis functions by the same procedure, to be described below;⁹ and (b) the coupling to T_2 modes alone has been found to be an incomplete model for other systems.¹¹

The total Hamiltonian H comprises three major contributions: the crystal-field or electronic Hamiltonian H_e ; the coupling or Jahn-Teller Hamiltonian H_{JT} ; and the vibrational or lattice Hamiltonian H_v . This can be written as

$$H = H_e + H_{JT} + H_v . \quad (1)$$

In the electronic Hamiltonian we consider the crystal-line field of tetrahedral coordination²¹ plus the spin-orbit interaction $\lambda \mathbf{S} \cdot \mathbf{L}$, where λ is expected to be about 100 cm^{-1} for the free Fe^{2+} ion while \mathbf{S} and \mathbf{L} represent the spin and orbital angular momenta respectively. We ignore the weak spin-spin interaction. The effect of the contributions to H_e is shown schematically in Fig. 1. The electronic eigenfunctions can be expressed either in terms of basis functions for angular-momentum operators⁵ or in terms of basis functions for the irreducible representations E and T_2 corresponding to the angular momentum quantum number 2.⁸ The latter seems to be a natural choice if H_{JT} is to show the explicit coupling to E vibrational modes. In Tables II and III we reproduce the electronic wave functions of Ref. 8, correcting for typographical er-

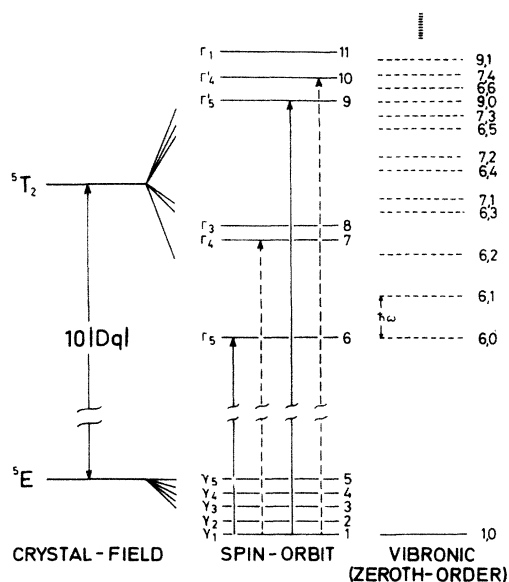


FIG. 1. Schematic of the splitting of the atomic 5D multiplet. On the left-hand side the crystal-field splitting is shown. In the central portion further splitting due to spin-orbit interaction is shown. The resulting electronic levels are labeled with notation corresponding to the irreducible representations of the group T_d . On the right-hand side the first few zeroth-order vibronic levels are shown for an arbitrary energy $\hbar\omega$ of the coupling mode. The notation l, N is such that l identifies the original electronic level in the sequential order given in the central part, while N is the total number of vibrational quanta. The discontinuous and continuous arrows correspond to allowed magnetic-dipole and electric-dipole transitions, respectively.

rors in two columns in the original work. We use capital letters for the upper multiplet while lower-case letters are used for the lower multiplet (see Fig. 1); the two basis functions for the E irreducible representation are denoted by θ and ϵ while the three basis functions for the T_2 irreducible representation are denoted by x , y , and z . In a ket the first symbol applies to the spin component while the second one applies to the orbital part.

The vibrational Hamiltonian corresponding to the two modes θ and ϵ of the E irreducible representation is taken in the usual harmonic approximation

$$H_v = \hbar\omega(a_\theta^\dagger a_\theta + a_\epsilon^\dagger a_\epsilon + 1) \quad (2)$$

in terms of creation (a^\dagger) and annihilation (a) operators for modes of energy $\hbar\omega$. The corresponding eigenfunctions can be characterized by means of the occupation numbers n and m for the modes θ and ϵ , respectively. Thus we have

$$H_v |nm\rangle = \hbar\omega(n+m+1) |nm\rangle. \quad (3)$$

The coupling Hamiltonian must be a scalar originating in a product between tensors of equal rank, one in the vibrational space and the other in the electronic space. The simplest form for the vibronic contribution to the total Hamiltonian can be written as

$$H_{JT} = K[(a_\theta^\dagger + a_\theta)D_\theta + (a_\epsilon^\dagger + a_\epsilon)D_\epsilon], \quad (4)$$

where the dimensionless electronic operators D_θ and D_ϵ have prescribed transformation properties which allow us to calculate the corresponding matrix elements.²² The coupling constant K is related to the so-called Jahn-Teller energy E_{JT} by the relationship

$$E_{JT} = \frac{K^2}{\hbar\omega}. \quad (5)$$

The next task is to define basis functions to perform a calculation which would yield the energies and eigenfunctions corresponding to the total Hamiltonian H . We choose to perform a complete diagonalization of H using the vibronic functions which can be constructed in the limit of a weak Jahn-Teller effect, where the Born-Oppenheimer approximation holds. We follow here the same method adopted by Maier and Scherz for Cu^{2+} in ZnS , in which symmetrized electronic functions like those in Tables II and III are combined with symmetrized vibrational functions by means of appropriate coefficients²² in order to give vibronic functions transforming according to the irreducible representations of the group T_d . Such zeroth-order vibronic functions can be denoted by $|\Gamma_i(\Gamma_j, N), s\rangle$, where N is the number of quanta of the vibrational part, namely,

$$N = n + m, \quad (6)$$

Γ_j represents the electronic multiplet, while Γ_i represents the final irreducible representation having s as the iso-

TABLE II. Eigenfunctions of the ten states belonging to the lower 5E electronic multiplet. N denotes the normalization factor ($g = \sqrt{3}$).

Irr. rep.	Function	N^2	$ \theta\theta\rangle$	$ \epsilon\theta\rangle$	$ x\theta\rangle$	$ y\theta\rangle$	$ z\theta\rangle$	$ \theta\epsilon\rangle$	$ \epsilon\epsilon\rangle$	$ x\epsilon\rangle$	$ y\epsilon\rangle$	$ z\epsilon\rangle$
γ_2	$ b\rangle$	2		-1				1				
	$ x\rangle$	4			-1					g		
γ_5	$ y\rangle$	4				-1					-g	
	$ z\rangle$	1					1					
γ_3	$ \theta\rangle$	2	-1						1			
	$ \epsilon\rangle$	2		1				1				
γ_4	$ u\rangle$	4			-g					-1		
	$ v\rangle$	4				g					-1	
γ_1	$ w\rangle$	1										1
	$ a\rangle$	2	1						1			

provements that could be reached by allowing the variation of all the four parameters are not considered in the present paper. For convenience we define a new index $m = i - 5$ ($i = 6, 7, 8, \dots$).

The most striking difference among the spectra of Fe^{2+} in various II-VI compounds is the relative intensities f_m/f_0 of the sharp zero-phonon absorption lines (f_0 is any preassigned intensity). We also find that the number of noticeable sharp lines also varies from compound to compound. Due to the sensitivity of the relative intensities we use this characteristic to find the region in the $E_{\text{JT}}-\hbar\omega$ plane which explains the experimental results.

The next sensitive characteristics are the upper energy levels which can be better handled as differences with respect to E_6 which is fixed by the value of the crystal-field parameter Dq . Let us define

$$\Delta_m = \Delta_{i-5} = E_i - E_6, \quad i = 6, 7, 8, \dots$$

We actually find for Fe^{2+} in CdTe that after the two free parameters are adjusted by means of a few line intensities, the Δ values agree well with experiment, thus providing an independent confirmation for the calculations.

For CdTe, the energies of the phonons that could be responsible for the vibronic coupling should correspond to those shown by the corresponding dispersion curves near the Brillouin-zone boundaries. From Table I we find that the range $30 \text{ cm}^{-1} \leq \hbar\omega \leq 60 \text{ cm}^{-1}$ satisfies this condition. For each $\hbar\omega$ in this range we try to find an E_{JT} that leads to approximately equal oscillator strengths for the first three absorption lines, namely, $f_1 \approx f_2 \approx f_3$. Actually it is convenient to define relative intensities f_m/f_0 , where f_0 is the minimum f_m among f_1, f_2 and f_3 . In this way, we avoid making assumptions for radial integrals involving wave functions and corrections to them for the different Dq values used along with the variation of $\hbar\omega$ and E_{JT} . Thus by taking ratios we cancel out other possible free parameters.

The results show that the criterion just defined, namely,

$$\frac{f_1}{f_0} \approx \frac{f_2}{f_0} \approx \frac{f_3}{f_0} \approx 1,$$

TABLE IV. Energy levels Δ_m and relative line intensities f_m/f_0 corresponding to the leading five vibronic states for different pairs of values $\hbar\omega$ and E_{JT} in the case of $\text{ZnS}:\text{Fe}^{2+}$. For each chosen value of $\hbar\omega$ we have searched for the value E_{JT} that gives the most approximate values to $\Delta_2 \approx 19 \text{ cm}^{-1}$ and $\Delta_3 \approx 39 \text{ cm}^{-1}$. It is clear that for $\hbar\omega \geq 50 \text{ cm}^{-1}$ this criterion as well as the condition of existence of just one dominant line are no longer satisfied. It is for the range $20 \text{ cm}^{-1} < \hbar\omega < 40 \text{ cm}^{-1}$ that further analysis can be carried out.

$\hbar\omega$ (cm^{-1})	E_{JT} (cm^{-1})	Δ_1	f_1/f_0	Δ_2	f_2/f_0	Δ_3	f_3/f_0	Δ_4	f_4/f_0	Δ_5	f_5/f_0
20	10	0	55.7	20	1.4	39	1.0	39	0.0	59	0.0
30	130	0	20.7	20	1.2	39	1.0	45	0.1	59	0.0
40	183	0	6.5	19	0.8	39	1.0	52	0.1	66	0.2
50	226	0	2.4	18	0.4	39	1.0	61	0.0	77	0.1
60	273	0	0.9	16	0.2	42	1.0	71	0.0	93	0.1
70	286	0	0.9	16	0.1	50	1.0	82	0.0	110	0.1
80	302	0	0.9	16	0.1	57	1.0	94	0.0	127	0.1
90	314	0	0.9	17	0.0	65	1.0	105	0.0	144	0.1
100	329	0	0.9	17	0.0	73	1.0	117	0.0	161	0.1

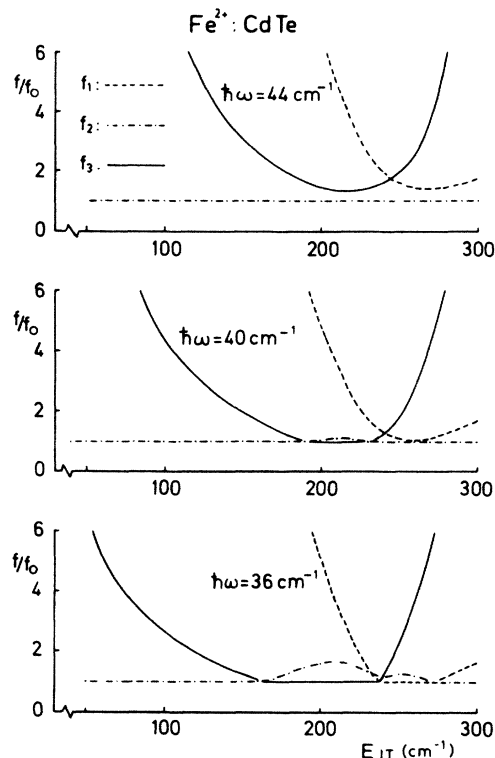


FIG. 2. Relative oscillator strengths for the first three zero-phonon lines as a function of the Jahn-Teller energy (E_{JT}). Three different values of the energy corresponding to the coupling phonon are illustrated.

narrows significantly the range for $\hbar\omega$. In Fig. 2 we show the variation of the relative oscillator strengths with respect to E_{JT} for three values of $\hbar\omega$. As a first approximation we could say that the energy of the coupling phonons must be in the range $36 \text{ cm}^{-1} \leq \hbar\omega \leq 44 \text{ cm}^{-1}$. It is interesting to notice that the associated value $E_{\text{JT}} \approx 240 \text{ cm}^{-1}$ does not change substantially in this range.

In the case of zinc sulfide the spectra show one very strong zero-phonon line and a succession of weak and

TABLE V. Energy levels Δ_m and relative lines intensities f_m/f_0 corresponding to the leading six vibronic states. The first row corresponds to results of our calculations. The second row represents the experimental values taken from Ref. 1 (ZnS:Fe²⁺). In the third row we present our interpretations.

	Δ_1	f_1/f_0	Δ_2	f_2/f_0	Δ_3	f_3/f_0	Δ_4	f_4/f_0	Δ_5	f_5/f_0	Δ_6	f_6/f_0
Calculations	0	6	48	0.04	105	1	137	0.00	178	0.2	200	0.00
Experimental	0	Strong			106	Medium			184	Medium		
Interpretation		(1-6)			(1-6) + TA	and (1-7)			(1-6) + LA			

very weak lines. It is almost impossible to make *a priori* assumptions about which of these are zero-phonon lines. Even if some reasonable assignments are tried the ratios of intensities will remain somewhat uncertain. So the strategy which proves to be successful for CdTe does not apply directly for ZnS.

Our first attempt was to obtain the appropriate values of $\hbar\omega$ and E_{JT} for the effective coupling phonon by adjusting the energy levels to the absorption lines at 2964 and 2984 cm⁻¹. These lines were previously interpreted^{1,6} as the zero-phonon lines (1-7) and (1-8) with $\Delta_2=19$ cm⁻¹ and $\Delta_3=39$ cm⁻¹, respectively. It is found that these conditions do not determine a point in the parameter space, but rather they actually define a sort of a ribbon. In Table IV we present an optimization of the adjustment $\Delta_2=19$ cm⁻¹ and $\Delta_3=39$ cm⁻¹. It is clear that for $\hbar\omega \geq 50$ cm⁻¹ it is not possible to satisfy both conditions simultaneously. Moreover Δ_3 never gets closer to 39 cm⁻¹ than the values reported in Table V. From this table we realize that a mathematical solution for these conditions exists. We performed careful calculations for the interval 20 cm⁻¹ $\leq \hbar\omega \leq 40$ cm⁻¹, increasing $\hbar\omega$ in steps of 1 cm⁻¹. At $\hbar\omega=25$ cm⁻¹ and $E_{JT}=85$ cm⁻¹ the fitting is good: $\Delta_1=0$; $\Delta_2=20$ cm⁻¹; $\Delta_3=39$ cm⁻¹; $f_1/f_0=57$; $f_2/f_0=1.3$; $f_3/f_0=1.0$; $f_4/f_0=0.01$; $f_5/f_0=0.02$; $f_6/f_0=0.01$. However, several other considerations tend to indicate that this is not a solution for the physical problem. From Table I we realize that the vibrational spectrum of ZnS spreads more to higher energies than the one of CdTe; the same comparison should apply to the vibronic spectrum of Fe²⁺ in these two compounds, which makes it difficult to accept small energy differences for zero-phonon lines without giving rise to several zero-phonon absorption lines of approximately similar intensities. On the other hand, coupling phonons of $\hbar\omega=25$ cm⁻¹ have a reduced wave vector of 0.2 (well inside the Brillouin zone).¹⁴ The wavelength of such a phonon extends for at least five unit cells so the relative displacements of the neighboring atoms would be quite small as to produce a vibronic coupling of importance. Moreover, the corresponding value of $E_{JT}=85$ cm⁻¹ is too far from the estimate¹ of 535 cm⁻¹ for the Jahn-Teller energy of Fe²⁺ in ZnS. Although this is only an estimate based on assumptions for the calculation of the oscillator strength of the (1-6) line, there is almost an order of magnitude of difference with respect to the calculated coupling energy. Finally, we would like to mention that the absorption spectra¹ taken at different temperatures (2.7, 9, and 21 K) do not seem to show a clear weakening of these lines in the same proportion as the (1-6) line at 2945 cm⁻¹. We are not in the position of providing any

calculations based on reasonable values for the coupling parameters in order to identify the weak absorptions at 2964 and 2984 cm⁻¹. Since these lines are present in the spectra of different samples all containing above 10¹⁹ atoms/cm³ of iron impurity we might think of iron-iron interactions as responsible for them. Actually such a mechanism was earlier invoked¹ as responsible for the lines at about 3010 and 3032 cm⁻¹ but later abandoned since these other two lines do not belong to all samples containing iron impurity. Still another possibility is to consider the coupling to longitudinal acoustic phonons in addition to the low-energy transverse acoustic phonons considered so far. Such treatment has been already performed for low numbers of vibrational quanta.⁶ We could equally extend it here to higher numbers of vibrational quanta by considering a second vibrational Hamiltonian of the same kind given by Eq. (2) as well as a second coupling Hamiltonian of the same kind given by Eq. (4). Since longitudinal phonons have frequencies of about thrice the corresponding frequencies of the transverse phonons, the corresponding absorption lines would lay beyond the region of the spectrum that we are presently studying. For this reason we will restrict ourselves to the coupling to a single set of *E* modes corresponding to the transverse acoustic branches near the Brillouin-zone boundaries. However, the method to be used is compatible with multiphonon coupling introducing a pair of parameters ($\hbar\omega', E'_{JT}$) for each different set of *E* modes considered. Alternatively, the second set of modes could be of *T*₂ symmetry corresponding to the discussion at the beginning of Sec. III which could again be treated by the same algorithm just outlined.

In order to perform calculations for ZnS we take into consideration some known properties of this system to make reasonable assumptions for $\hbar\omega$ and E_{JT} . First, we maintain the idea that the coupling phonons must be found near the boundaries of the Brillouin zone in order to produce the necessary relative displacements within the unit cell; the lowest-energy phonons satisfying this criterion belong to the acoustic branches of ZnS whose energies are given in Table I, namely, 70 cm⁻¹ $\leq \hbar\omega \leq 120$ cm⁻¹. Second, we believe that the points in reciprocal space responsible for the vibronic coupling in CdTe are about the same as in ZnS (and other materials with the same point group); by superposing the dispersion curves of CdTe and ZnS one finds that the frequency of 40 cm⁻¹ of the former corresponds to the frequency of about 100 cm⁻¹ of the latter. Third, it is expected that the vibronic coupling in ZnS is less effective than in CdTe;⁶ the Jahn-Teller energy for ZnS cannot be larger than the one in CdTe. Fourth, calculations already performed⁸ for the

far-infrared spectra showed that the Jahn-Teller effect in ZnS plays a negligible role. With these assumptions both cases CdTe:Fe²⁺ and ZnS:Fe²⁺ can be handled in the same way.

V. RESULTS AND DISCUSSION

The discussion of the results will be organized in the following way: (a) Comparison with experimental results and previous interpretations for Fe²⁺ in CdTe; (b) comparison with experimental results and previous interpretations for Fe²⁺ in ZnS; (c) analysis of the method and its possible extensions.

(a) Fe²⁺ in CdTe presents optical properties in the infrared which can be associated with states whose wave functions and energies can be accounted for by means of vibronic coupling.

The method and the previously imposed conditions succeed in giving exactly three zero-phonon absorption lines of about the same intensity, in perfect agreement with experiments. This is shown in Fig. 2 and was already discussed in Sec. IV. The appropriate parameter values are found to be $\hbar\omega = 40 \text{ cm}^{-1}$ for the coupling phonon and $E_{JT} = 240 \text{ cm}^{-1}$ for the Jahn-Teller energy. With no free parameters left, straight calculations of other properties are performed and compared with experiments.

The line intensities for the three following absorption lines can be read from Fig. 3 where the reading for $E_{JT} = 240 \text{ cm}^{-1}$ (shown with an arrow) indicates intensities of about $\frac{1}{5}$ with respect to the first three lines. On the other hand, Fig. 4 shows that for $N = 10$ vibrational quanta, a clear asymptotic behavior of all the intensities is reached, which allows us to draw firm conclusions based on them. The low intensities of the lines next to the set of three leading lines makes it rather difficult to identify such absorptions. This agrees well with the experiment as no other clear zero-phonon line is observed.

The energies of the vibronic levels are shown in Fig. 5 in the form of differences Δ_m defined earlier, with respect to the number of vibrational quanta considered in the diagonalization of the vibronic Hamiltonian. (Notice that $\Delta_1 = 0$).

It is clear that Δ_2 and Δ_3 show convergence to an asymptotic behavior which is in good agreement with the observed energies shown on the extreme right ($N \rightarrow \infty$). No such clear asymptotic behavior is observed for Δ_4 , Δ_5 , and Δ_6 after 10 vibrational quanta are considered. Probably as many as 20 vibrational quanta would be necessary in order to reach convergence. However, even if such calculation is performed it is very unlikely that these extra zero-phonon lines can be seen due to the low intensities already discussed and due to the range of energies that they would have, where strong competition coming from phonon-assisted transitions would mask them. Actually we believe that the experimental lines at Δ_4 , Δ_5 , and Δ_6 are primarily one-phonon lines as already interpreted.⁵

Finally, let us compare the values of the two adjustable parameters with other experimental evidence. Firstly, $\hbar\omega = 40 \text{ cm}^{-1}$ is in good correspondence with the lattice dynamics of CdTe as seen from Table I and it lies between the values of 29 and 53 cm^{-1} used for TA(L) and

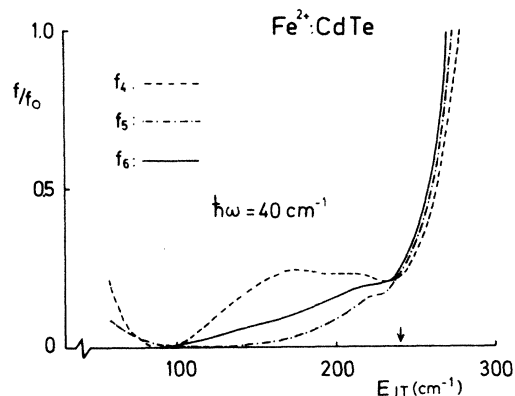


FIG. 3. Relative oscillator strengths for the next three possible absorption lines as a function of the Jahn-Teller energy (E_{JT}). We still normalize with respect to the lowest oscillator strength corresponding to the three leading absorptions shown in Fig. 2.

TA₂(K), respectively, in order to explain the phonon-assisted lines.⁵ Secondly, $E_{JT} = 240 \text{ cm}^{-1}$ is close to 255 cm^{-1} estimated from assumptions in relation to the absolute oscillator strengths.¹

(b) Fe²⁺ in ZnS shows absorptive spectra with a pattern quite different as compared with the same ion in CdTe. The plausible argument presented in Sec. IV allows us to justify an energy of 100 cm^{-1} for the coupling phonon. We discuss now the results based on this assumption considering the existence of just one dominant zero-phonon line at 2945 cm^{-1} .

In Fig. 6 we present the leading six oscillator strengths as functions of the Jahn-Teller energy for the present value $\hbar\omega = 100 \text{ cm}^{-1}$. We look here for just one dominant zero-phonon absorption line corresponding to the (1-6) transition. This criterion excludes right away all values above 240 cm^{-1} for E_{JT} , where several absorption lines should be observed. It is interesting to notice that f_2 is always weak which makes f_3 the first candidate for an extra zero-phonon line. The energies of the leading three vibronic levels corresponding to the upper ⁵T₂ triplet are

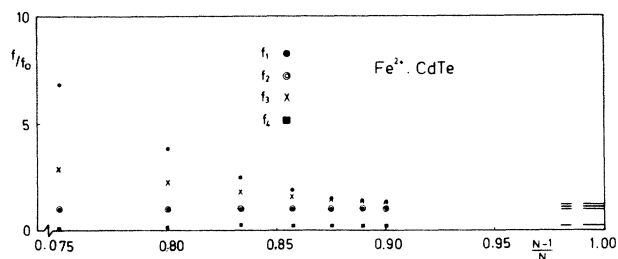


FIG. 4. Variation of relative oscillator strength with the number of vibrational quanta N . The dots represent direct calculations for $\hbar\omega = 40 \text{ cm}^{-1}$ and $E_{JT} = 240 \text{ cm}^{-1}$. The plotting is actually performed with respect to $(N-1)/N$ which allows us to schematically illustrate the experimental results on the extreme right. It is clear that for $N = 10$ the calculated intensities are both stable and converging to the expected values.

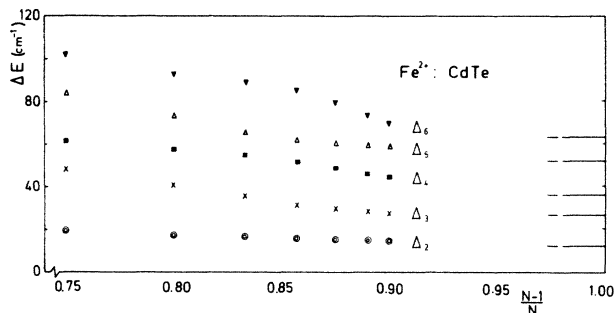


FIG. 5. Variation of the energy levels with the number of vibrational quanta N . The dots represent direct calculations for $\hbar\omega=40\text{ cm}^{-1}$ and $E_{JT}=240\text{ cm}^{-1}$. As in Fig. 4 the plotting is performed with respect to $(N-1)/N$. (The dots for $\Delta_1=0$ are omitted.)

presented in Fig. 7 as a function of E_{JT} for the fixed value of $\hbar\omega=100\text{ cm}^{-1}$ ($\Delta_1=0$). It is clear that coexistent vibronic levels at $\Delta_2=19\text{ cm}^{-1}$ and $\Delta_3=39\text{ cm}^{-1}$ (indicated by short arrows in Fig. 7) are not possible. The convergence of both oscillator strengths and energy levels with respect to the number of vibrational quanta N is reached much faster than the cases shown in Figs. 4 and 5 for CdTe, so we will report results with $N=10$ without further reference to it.

We examine Fig. 7 with attention to Δ_3 which is the best candidate to give rise to an observable zero-phonon absorption. At $E_{JT}=200\text{ cm}^{-1}$ we read $\Delta_3=105\text{ cm}^{-1}$ which is close to the observed transition at about 106 cm^{-1} indicated by the long arrow in Fig. 7. The possible energy differences and intensities for $\hbar\omega=100\text{ cm}^{-1}$ and $E_{JT}=200\text{ cm}^{-1}$ are compared in Table V. The lines at 106 and 184 cm^{-1} were previously interpreted^{1,6} due to phonon-assisted transitions and we still believe this is the most important process that accounts for these absorptions. If we assume that the phonon-assisted transitions

are due to phonons originating in the same reduced wave vectors as compared with CdTe, then from Table I we find that phonon energies of ≈ 90 and $\approx 195\text{ cm}^{-1}$ should be appropriate for ZnS. From this analysis we can make the proposal contained in the third line of Table V. The combined effect of zero-phonon plus phonon-assisted transitions could produce a rather wide and round line as is the experimental case. This combination would also explain the sharpness and slight shifting of the line at Δ_3 as temperature is raised indicating the prevalence of the phonon assisted over the zero-phonon transitions. The zero-phonon line at Δ_5 is too weak to introduce any significant modification to the $(1-6) + \text{LA}$ line and the corresponding $(2-6) + \text{LA}$ that arises with higher temperatures.

Thus the values of $\hbar\omega \approx 100\text{ cm}^{-1}$ and $E_{JT} \approx 200\text{ cm}^{-1}$ give a good and consistent explanation for the vibronic coupling that slightly modulates the spectrum of Fe^{2+} in ZnS at low temperatures.

(c) The method we have used is based on the analysis of the intensities corresponding to the absorption transitions at very low temperatures (zero-phonon lines originating from the ground state). This criterion applied to Fe^{2+} in CdTe gives the correct absorbed energies and the correct intensities of all other possible lines as a direct result of a calculation. Moreover, the corresponding values for $\hbar\omega$ and E_{JT} are within the expected range. On the other extreme is the case of ZnS where just one zero-phonon line is observed at low temperatures. However, good results for the possible transitions are obtained after a reasonable value of $\hbar\omega$ is picked (justifiable from lattice-dynamics considerations in analogy with CdTe). We believe this method can be used and extended to other crystals of the same point-group symmetry such as (ZnSe, ZnTe, CdS, etc.) with Fe^{2+} or other transition-element impurities. We have chosen here what seems to be the two extreme cases: CdTe for which a substantial Jahn-Teller effect is present providing two extra zero-phonon lines and ZnS where a very weak Jahn-Teller effect provides an almost un-

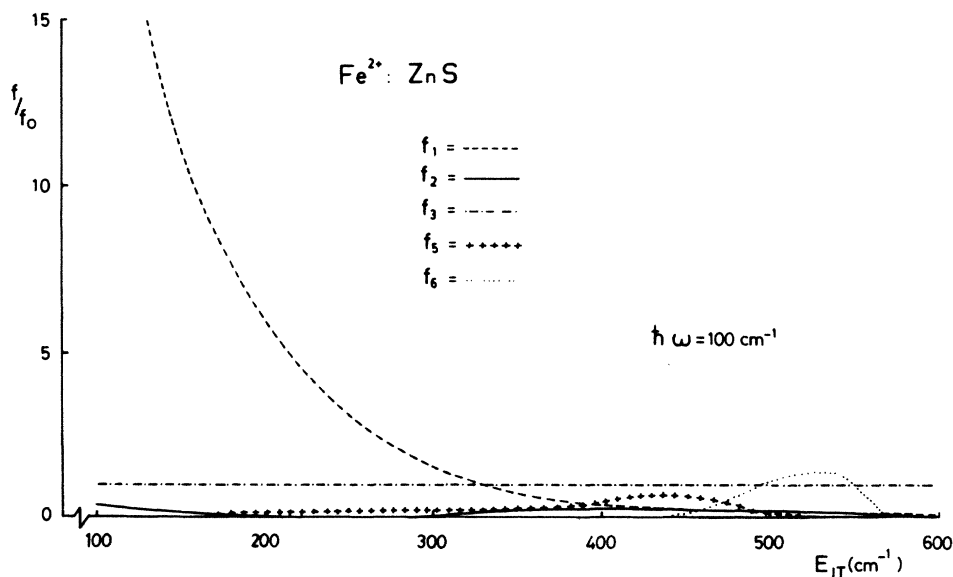


FIG. 6. Relative oscillator strength for the first six possible zero-phonon lines as a function of the Jahn-Teller energy. In this case we simply define $f_0=f_3$ for convenience.

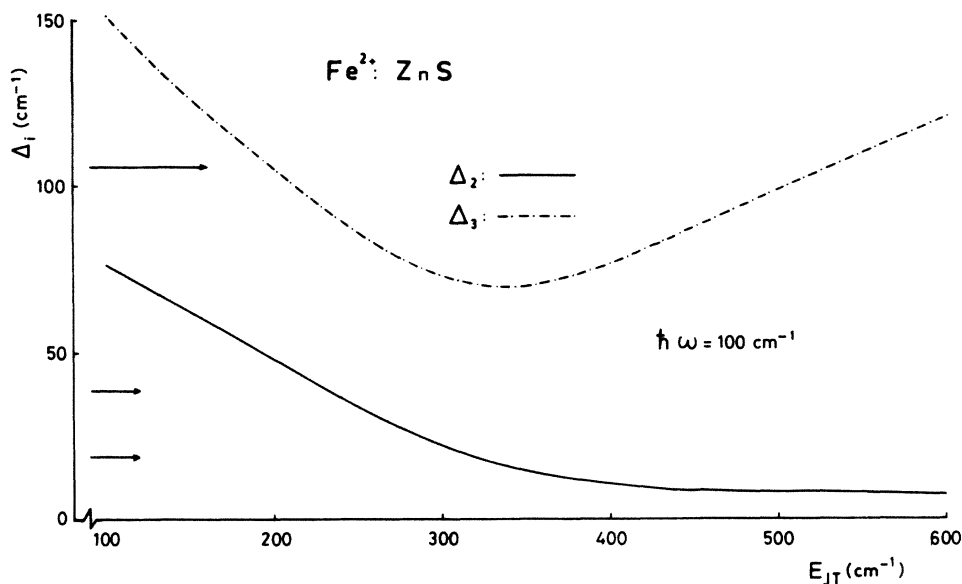


FIG. 7. Energy of the three leading vibronic levels as a function of the Jahn-Teller energy ($\Delta_1=0$). Short arrows indicate two weak experimental lines formerly interpreted as zero-phonon lines. The low arrow indicates an experimental line which can be accounted in part as due to vibronic coupling.

noticeable extra zero-phonon line. Any other case would probably be in between these two or could be a slight extension beyond the coupling studied in the case of Fe^{2+} in CdTe. Of course, the method can be improved by considering aspects such as correction to the simple crystal-field theory used here, corrections to the free-ion spin-orbit parameter, coupling to more than one kind of phonons and diagonalization of larger matrices containing vibronic states with increasing values of vibrational quanta beyond $N=10$. However, we believe the basic role of the vibronic coupling is better understood without optimal numerical fittings.

VI. CONCLUDING REMARKS

Several conclusions can be obtained from the preceding quantitative analysis and its application to two particular cases.

First, the vibronic coupling is responsible for the appearance of extra zero-phonon lines in the spectra of magnetic impurities substituting in II-VI compounds. In the extreme case of ZnS formed by light atoms an almost negligible JT effect is present and a dominant line is observed. On the other hand, for the heavier CdTe a quite noticeable JT effect is possible and three zero-phonon lines are predicted.

Second, the values of the effective coupling parameters are better found by looking at the relative intensities of the absorbed lines rather than the energies of the absorbed photons. Where there are several zero-phonon lines the problem has too much information as more than two linear independent conditions arise. In such cases we use the line intensities to determine $\hbar\omega$ and E_{JT} , and then the other experimental results are simply compared with straight calculations.

Third, the number of vibrational quanta can be studied by looking at the convergence of the results to the stable values that correspond to the experimental data. In this way a criterion can be established in advance in order to increase the total number of vibrational quanta N up to a point where the solutions are practically independent of N .

Fourth, the case of CdTe: Fe^{2+} is an example of too much information. Three quite distinct zero-phonon lines giving two relative intensities determine the values $\hbar\omega=40\text{ cm}^{-1}$ and $E_{JT}=240\text{ cm}^{-1}$, reaching clear convergence for $N=10$. Under these conditions several other properties are calculated and directly compared with experiments. The low intensities of the other possible zero-phonon lines agree well with the fact that only three lines are observed. The corresponding energy-level scheme is in agreement with the energies of the absorbed photons. The value $\hbar\omega=40\text{ cm}^{-1}$ corresponds well with lattice dynamics of CdTe.¹⁴ The value $E_{JT}=240\text{ cm}^{-1}$ is close to approximate estimates made previously.¹

Fifth, the case of ZnS: Fe^{2+} is an example of not enough information. Just one zero-phonon line gives no place to relative intensities or relative energy differences. If the assumption is made that the coupling phonons are given both in CdTe and ZnS by the same reciprocal-lattice vectors then the phonon energy can be asserted to be about 100 cm^{-1} for ZnS: Fe^{2+} . The JT energy is then adjusted to reproduce the characteristics of the lone zero-phonon line. The value of $E_{JT}=200\text{ cm}^{-1}$ gives just one dominant line and is within an order of magnitude of previous estimates for E_{JT} .¹ The convergence is reached here for $N=6$.

Sixth, the method and the results could be improved by considering other crystal-field techniques. In particular

the value of the spin-orbit parameter is surely quenched by the Jahn-Teller effect so the value of $\lambda = 100 \text{ cm}^{-1}$ is probably too large.²³ However, we prefer to consider a standard crystal-field approach in order to perform the variations in the vibronic coupling alone.

Seventh, the generality and simplicity of the method allows its application to other similar systems. At the moment of writing this last conclusion initial and crude results for other II-VI compounds with iron impurities show also good agreement with experimental data. However, numerical calculations with larger matrices for

larger values of N are still necessary in order to perform the corresponding analysis.

ACKNOWLEDGMENTS

Two of the authors (J.R.-I. and M.A.d.O.) would like to thank Dirección de Investigación de la Universidad de Concepción for the funding of the Research Project that allowed their work on this area. The other author (E.E.V.) wants to thank Dirección de Investigación de la Universidad de la Frontera for partial support.

-
- ¹G. A. Slack, F. S. Ham, and R. M. Chrenko, *Phys. Rev.* **152**, 376 (1966).
²G. A. Slack, S. Roberts, and F. S. Ham, *Phys. Rev.* **155**, 170 (1967).
³G. A. Slack and B. M. O'Meara, *Phys. Rev.* **163**, 335 (1967).
⁴J. M. Baranowski, J. W. Allen, and G. L. Pearson, *Phys. Rev.* **160**, 627 (1967).
⁵G. A. Slack, S. Roberts, and J. T. Vallin, *Phys. Rev.* **187**, 511 (1969).
⁶F. S. Ham and G. A. Slack, *Phys. Rev. B* **4**, 777 (1971).
⁷J. T. Vallin, *Phys. Rev. B* **2**, 2390 (1970).
⁸E. E. Vogel and J. Rivera-Iratchet, *Phys. Rev. B* **22**, 4511 (1980).
⁹F. S. Ham, W. M. Schwarz, and M. C. M. O'Brien, *Phys. Rev.* **185**, 548 (1969).
¹⁰H. Maier and U. Scherz, *Phys. Status Solidi B* **62**, 153 (1974).
¹¹S. M. Uba and J. M. Baranowski, *Phys. Rev. B* **17**, 69 (1978).
¹²K. Kunc, *Ann. Phys.* **8**, 319 (1973).
¹³J. M. Rowe, R. M. Nicklow, D. L. Price, and K. Zanio, *Phys. Rev. B* **10**, 671 (1974).
¹⁴N. Vagelatos, D. Wehe, and J. S. King, *J. Chem. Phys.* **60**, 3613 (1974).
¹⁵M. Vandevyver and P. Plumelle, *J. Phys. Chem. Solids* **38**, 765 (1977).
¹⁶C. Patel, W. F. Sherman, and G. R. Wilkinson, *J. Mol. Struct.* **79**, 297 (1982).
¹⁷T. Soma and H.-Matsuo Kagaya, *Solid State Commun.* **46**, 773 (1983).
¹⁸T. Soma and H.-Matsuo Kagaya, *Solid State Commun.* **46**, 885 (1983).
¹⁹H.-Matsuo Kagaya and T. Soma, *Phys. Status Solidi B* **124**, 37 (1984).
²⁰M. D. Sturge, in *Solid State Physics*, edited by F. Seitz, D. Turnbull, and H. Ehrenreich (Academic, New York, 1967), Vol. **20**, p. 91.
²¹M. T. Hutchings, in *Solid State Physics*, edited by F. Seitz and D. Turnbull (Academic, New York, 1964), Vol. **16**, p. 227.
²²G. F. Koster, J. O. Dimmack, R. G. Wheeler, and H. Statz, *Properties of the Thirty-Two Point Groups* (MIT University Press, Cambridge, MA, 1963).
²³I. B. Bersuker, *The Jahn-Teller Effect and Vibronic Interactions in Modern Chemistry* (Plenum, New York, 1984).